



## PRELIMINARY FINITE ELEMENT MODELLING OF FOUR BRICK UNIT SPECIMENS SUBJECTED TO BENDING

Yan Han<sup>1</sup>, Mark J. Masia<sup>2</sup>, Stephen J. Lawrence<sup>3</sup> and Adrian W. Page<sup>4</sup>

<sup>1</sup> Postgraduate, [yan.han@studentmail.newcastle.edu.au](mailto:yan.han@studentmail.newcastle.edu.au)

<sup>2</sup> Lecturer, [mark.masia@newcastle.edu.au](mailto:mark.masia@newcastle.edu.au)

<sup>3</sup> Conjoint Professor, [spl@bigpond.net.au](mailto:spl@bigpond.net.au)

<sup>4</sup> Professor, [adrian.page@newcastle.edu.au](mailto:adrian.page@newcastle.edu.au)

Faculty of Engineering and Built Environment, The University of Newcastle, Callaghan NSW 2308, Australia

### ABSTRACT

The paper presents a 3D non-linear finite element micro model capable of simulating the behaviour of masonry specimens under the simultaneous combination of horizontal and vertical bending moments and vertical compressive force. Such two way bending actions arise in masonry wall panels when supported on two or more adjacent edges and subjected to out-of-plane loads. The numerical results are compared to the results of preliminary laboratory tests using 4-unit brick specimens subjected to such actions as well as analytical predictions. In this paper, only tests in which specimens were subjected separately to one way vertical and one way horizontal bending, with vertical axial compression, were considered. The model described in this paper, which incorporates the mortar thickness and brick failure, is a refinement of the model published previously [1]. The next stage of an on going research project will focus on biaxial bending behaviour in which masonry specimens are subjected to vertical and horizontal bending moments and vertical compression simultaneously. It is hoped that such research will ultimately lead to the development of more rational design procedures for face loaded masonry walls.

**KEYWORDS:** unreinforced masonry, biaxial, bending, non-linear modelling, torsion

### INTRODUCTION

Masonry walls, whether being used as vertical load bearing elements, shear walls or as non-structure infill, are inevitably required to resist out-of-plane loads due to the action of wind, earthquakes or water or earth pressure. Despite many efforts over the past several decades to investigate the out-of-plane behaviour of masonry panels, little fundamental understanding has been achieved due to the complexity exhibited, as masonry is both anisotropic and non-homogeneous. Of particular interest is the case that arises when the walls are supported on two or more adjacent edges. Under these conditions, the masonry is subjected to a state of two way, or biaxial, out-of-plane bending combined with vertical in-plane compression due to the self-weight of the wall and any superimposed gravity loads. The distribution of the bending moments

in the horizontal and vertical directions depends on the wall geometry and support conditions and varies across any given wall panel as does the vertical preload.

Mortar joints in masonry are planes of weakness. Failure under biaxial bending can occur by:

- fracture of bed joints (vertical bending  $M_v$  dominant, Figure 1(i)) or
- fracture of perpend and masonry units (Figure 1(ii)) or toothed or stepped failures through perpend and bed joints (Figure 1(iii)) (horizontal bending  $M_h$  dominant) or
- fracture along diagonal stepped crack paths through the bed and perpend joints (combination of  $M_v$ ,  $M_h$  and a twisting moment  $M_{hv}$ , Figure 1(iv)).

Typical experimentally observed failure patterns in full wall panels are shown in Figure 2.

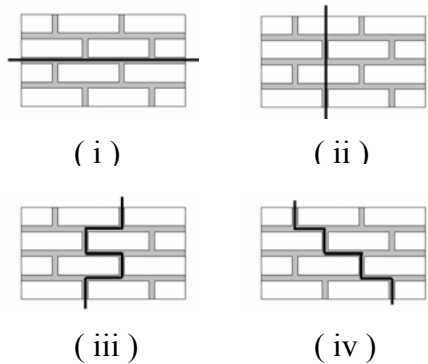


**Figure 1 - Possible Failure Modes under Biaxial Bending**

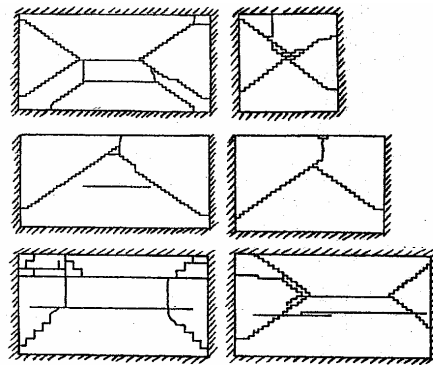


**Figure 2 - Examples of Wall Crack Patterns (2)**

Intensive research has been conducted to study the behaviour of walls under biaxial bending [2, 3,4] and different approaches to the design of walls under such loading have been developed and adopted by individual countries. The approaches available vary considerably and the theories they are based on either under or over estimate the flexural strength of the masonry walls under out-of-plane loading. This is due to the fact that these approaches are either totally or partially empirical and can only be applied to limited tested scenarios [5]. Lawrence and Marshall [6] note that “no completely rational method has yet been developed” and that “further research is necessary to develop a fully rational biaxial bending failure model that can predict behaviour under any simultaneous combination of bending moments in the two principal directions, along with a superimposed compression force along the bed joints”.

Current research at The University of Newcastle aims to obtain a better understanding of the complex behaviour of masonry walls under biaxial bending. Initially this will be achieved by experimentally and numerically studying “single joint” 4-unit specimens of masonry subjected simultaneously to horizontal and vertical bending as well as vertical pre-compression (Figure 3). This paper describes the numerical approach adopted in the project. As a starting point, the numerical analyses are compared with preliminary experimental results which consider separately vertical bending and horizontal bending, each combined with vertical compression. Although the numerical model is capable of simulating biaxial bending in which masonry specimens are subjected to vertical and horizontal bending moments and vertical compression

simultaneously, insufficient experimental data exists at this stage to allow comparison for such cases. This will form the focus of future work.

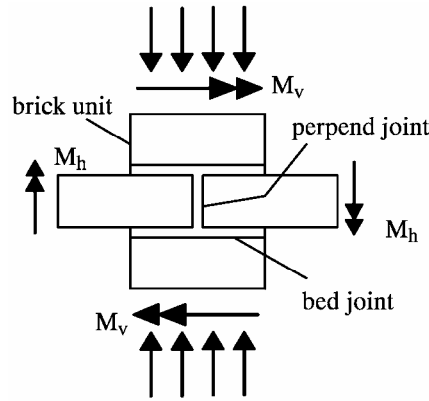


**Figure 3 – Four Brick Unit Biaxial Bending Test Specimen**

### MODEL DESCRIPTION

Failure in masonry is generally confined to the mortar joints as well as a potential vertical failure interface at the mid-length of the masonry unit if the bricks are laid in stretcher bond. In this paper, a micro modelling strategy is used in which both bricks and mortar are represented with 3D linear elastic continuum elements and the bond between brick and mortar at the bed and perpend joints, and the potential brick vertical failure interface are represented by non-linear contact interface elements. This allows the numerical representation of crack formation and propagation at these interfaces [7, 8]. For each pair of contacted surfaces, an appropriate interface law is applied to govern the interaction of the surfaces. While in a real wall joint failure may also be due to the cracking within the mortar itself, in this paper emphasis is on the bond at the mortar/brick interface.

The contact relationship defines both tangential and normal interactions. The tangential behaviour follows the Mohr-Coulomb rule with a frictional coefficient and cohesion. The normal contact is considered as being elastic brittle under tensile forces but elastic with infinite capacity under compressive forces. The bed and perpend joints are assumed to have the same flexural and torsional capacities. Results reported by Willis *et al.* [9] indicate that this assumption is justified. By using these non-linear contact relationships at the mortar joints and brick mid-length the model is able to capture the essentially elastic pre-cracking and brittle and/or frictional post-cracking behaviour observed experimentally.

Abaqus commercial finite element software [10] is employed to implement the model. The shear strength between the contacted surfaces is related to the normal stress through the classic Mohr-Coulomb rule:

$$\tau = \mu\sigma + c \quad \text{Equation 1}$$

where  $\tau$  is the tangential shear strength,  $\mu$  is a frictional coefficient,  $c$  is cohesion and  $\sigma$  is the normal stress (positive for compression and negative for tension). Since the default tangential

contact relationship available in Abaqus models frictional resistance only (elastic plastic), it had to be modified in this study to include the cohesion component as well as post peak softening.

Across each contact surface, the shear resistance is assumed to be isotropic. The shear stress increases linearly as the relative displacement of adjacent nodes on the mating contact surfaces increases (Figure 4). The elastic stiffness  $k$  is taken as  $\tau_{crit}/\gamma_{crit}$  where  $\tau_{crit}$  is the shear strength calculated using Equation 1 and  $\gamma_{crit}$  represents the maximum allowable elastic slip. When the shear stress reaches the critical shear strength  $\tau_{crit}$ , the cohesion  $c$  is reduced exponentially to zero as the relative node displacement further increases. This represents the softening stage where the crack is forming and the element surfaces of the contact pair start to show relative movement. Beyond this point only frictional force (constant shear stress  $\tau_{res}$ ) dominates the relative tangential movement of the nodes of the pair. The same coefficient of friction  $\mu$  is used to describe the pre-crack (Equation 1) and post crack frictional shear resistance.

In the normal direction, the tensile stress increases linearly until it reaches the mortar flexural tensile strength, after which the surfaces of the pair separate from each other and the normal stiffness drops to zero instantly (Figure 5). This represents the opening of the nodes of the contact pair. It should be pointed out that Abaqus software provides a default normal contact model to simulate this tensile behaviour. It is not ideal because the failure moment for the simulation of the 4-unit specimens under vertical bending  $M_v$  is sensitive to the initial step length chosen. For this study, careful adjustment in the step length was made to obtain the overall moment versus rotation response that represents the independent analytical predictions as closely as possible. However, the robustness of the numerical implementation of the normal contact model is being investigated further.

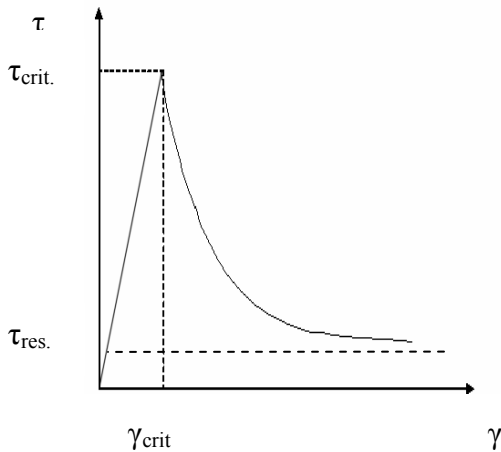


**Figure 4 – Tangential Shear Strength Versus Shear Displacement**

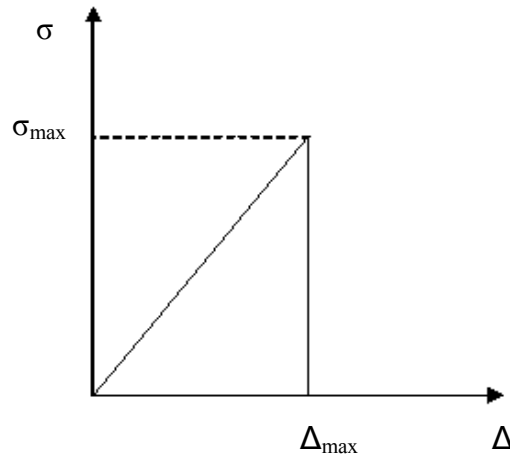


**Figure 5 – Normal Tensile Strength Versus Normal Displacement**

## EXPERIMENTAL PROGRAM

The experimental results used for the current study were obtained from two preliminary series of tests using an experimental rig described previously [11]. In brief, the apparatus is capable of subjecting “single joint” specimens of 4 brick units (Figure 3) to various combinations of vertical compression and horizontal ( $M_h$ ) and vertical ( $M_v$ ) out-of-plane bending moments. Such two

way bending actions arise in the mortar joints of masonry wall panels when supported on two or more adjacent edges and subjected to out-of-plane loads. The actuators imposing the compression and moment actions can be independently controlled in either a load control or displacement control mode.

The testing procedure consists of firstly imposing any vertical compression and then holding this constant (load control). The moments  $M_v$  and  $M_h$  are then slowly incremented simultaneously at a predetermined ratio  $M_v:M_h$ . The specimens are instrumented with displacement potentiometers and the tests are continued past specimen failure to record any post peak response. In the presence of vertical compression there is typically a post peak (post cracking) moment resistance under the action of any combination of moments ( $M_v$  only,  $M_h$  only or  $M_v$  and  $M_h$ ). In the following discussion the “peak” moments are those at which the specimen fails by joint or brick rupture and the “residual” moments are the continued post cracking moment resistance under the action of the vertical compression and/or torsional frictional sliding as the specimen displacement is continued. Although the actuators applying the moments were operated in displacement control, elastic energy stored in the torque shafts applying the moments resulted in sudden unloading upon specimen failure making it impossible to accurately record the full softening behaviour of the specimens. However, it was still possible to obtain values of residual moment.

## **EXPERIMENTAL AND NUMERICAL RESULTS FOR VERTICAL BENDING $M_v$**

*Experimental ( $M_v$  tests).* 15 specimens were tested under vertical compression combined with moment  $M_v$  to study the vertical bending behaviour under increasing levels of pre-compression, particularly the post cracking behaviour which cannot be observed in bond wrench or beam tests. Three specimens were tested at each of five levels of pre-compression: 0, 1.25, 2.5, 3.75 and 5 kN, corresponding to compressive stresses of 0, 0.05, 0.10, 0.15 and 0.20 MPa, respectively. The specimens were constructed using Austral extruded solid clay bricks (230mm long x 110mm thick x 76mm high) and 10mm thick joints using 1:0:7 (C:L:S by volume) mortar with 5% replacement of sand with ground limestone (to attempt to retain mortar workability). Accompanying these tests, bond wrench tests were conducted in accordance with AS 3700-2001 [12] using the same bricks and mortar batch (10 joints were tested, resulting in a mean flexural bond strength of 1.22 MPa, std dev. 0.13 MPa).

*Numerical Modelling ( $M_v$  tests).* The numerical model was used to simulate the above tests. Figure 6 shows the finite element mesh used to model the brick and mortar. As both the geometry of the specimen and imposed actions are symmetric, only half of the specimen was modelled. The brick units were modelled with  $8 \times 4 \times 4$  elements (number of elements long  $\times$  number of elements thick  $\times$  number of elements high). The middle part of the upper and lower bricks have finer meshes to match the nodes with those from the perpendicular joint. In the direction of the thickness of the mortar, two layers of elements were adopted. The mean flexural strength determined using the bond wrench tests was used as input data for the parameter representing the tensile bond strength between interfaces of mortar and brick in the numerical model. It was also used in the analytical model described below to calculate the failure moment of the specimen. Ideally a tensile bond strength determined from a direct tension test may be more appropriate and this will be investigated during the next series of tests.

*Analytical Modelling ( $M_v$  tests).* A simple analytical method was used to provide an independent check on the numerical model. The method uses simple beam theory to calculate the peak moment to cause joint cracking and uses statics to calculate the residual moment required to balance the moment due to the vertical compressive force after the bed joint has cracked and opened (assuming brick rotation about the compression edge). Figure 7 illustrates the actions present upon the specimen when it was subjected to vertical bending and compression forces.

The peak moment was calculated as:

$$M_{v,\text{peak}} = [\sigma_f + (F + W)/A] \times Z \quad \text{Equation 2}$$

The residual moment was calculated as:

$$M_{v,\text{res}} = (F + W) \times t/2 \quad \text{Equation 3}$$

where  $\sigma_f$  is the flexural tensile strength,  $F$  is the vertical compressive force,  $W$  is the weight of one brick,  $A$  is the area of the brick surface (or bed joint area),  $Z$  is the section modulus of the bed joint, and  $t$  is the thickness of the brick.

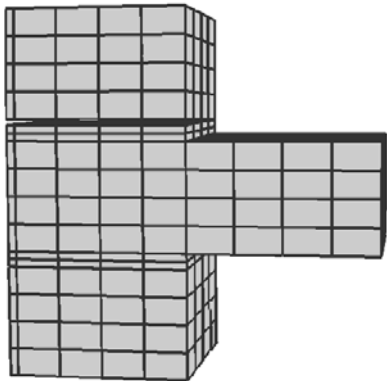


**Figure 6 – Finite Element Mesh and Failure in Vertical Bending**

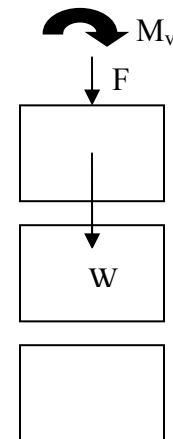


**Figure 7 – Actions in Vertical Bending**

*Results and Discussion ( $M_v$  tests).* In all tests specimen failure occurred by rupture of either the upper or lower bed joint, usually at the brick mortar interface. In cases where vertical compressive force was applied, the specimens continued to support a residual moment after cracking. The numerically predicted failure behaviour of the four brick unit specimens under vertical bending is illustrated in Figure 6 and agrees with the experimental observations. Figure 8 compares the peak (failure) moments and residual moments for various levels of vertical pre-compressive stress as obtained from the experiment, analytical and numerical analyses.

It can be seen from Figure 8 that the numerical and analytical models give predictions of the peak and residual moments, which agree very closely. However, both methods significantly overestimate the experimentally observed peak moments and underestimate the experimental residual moments. The reason for this is still unclear. Subsequent checks of the test apparatus using a calibrated steel specimen have shown that the values of  $M_v$  recorded using the test

apparatus are different to values measured directly on the calibrated specimen. Also, the presence of the clamp applying  $M_v$ , even though it is counterweighted, appears to affect the vertical compressive force applied to the specimen. The authors believe that the problems may be due to the way the  $M_v$  clamp is counterweighted, but at the time of writing this is still being investigated. However, it can be concluded that the disparity between experimental and numerical/analytical observations for the case of vertical bending appears to result from experimental error rather than errors in the numerical or analytical approaches.

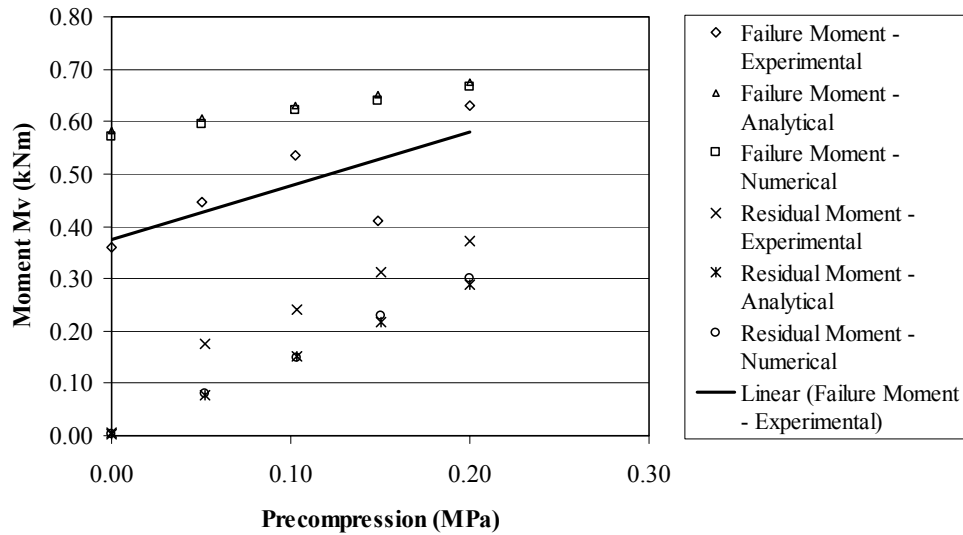


**Figure 8 – Vertical Bending Moment Versus Vertical Pre-compression**

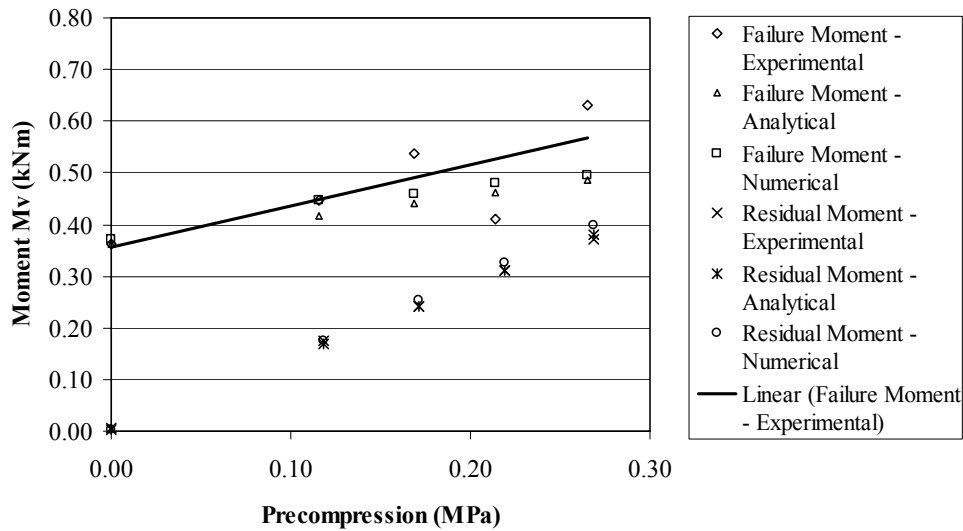


**Figure 9 – Vertical Bending Moment Versus Pre-compression after Correction**

Some attempt was made to correct for these errors. In the case of post cracking residual moments, the error in  $M_{v,res}$  was observed to be approximately constant at around 0.09 kNm, regardless of the pre-compression level (Figure 8). This is equivalent to 1.66 kN extra

compression force being added at the centre of the specimens. Therefore, the compressive forces were corrected to 0, 3.91, 4.16, 5.41, 5.71 kN, respectively. Also, the mean flexural tensile strength of 1.22 MPa from the bond wrench test appeared to be relatively high for the mortar type of 1:0:7. So the analytical and numerical predictions of peak  $M_v$  values were repeated using a flexural tensile strength of 0.76 MPa, which is the mean failure flexural stress obtained from the 4-unit specimen tests subjected to vertical bending without pre-compression. As shown in Figure 9, after correction both the analytically and numerically predicted residual and peak moments are much closer to the experimental values and fit the experimentally observed trends. This gives confidence that when the apparently systematic errors with the testing apparatus are corrected and a greater number of replicates are tested, close agreement with the numerical and analytical predictions will be possible.

### EXPERIMENTAL AND NUMERICAL RESULTS FOR HORIZONTAL BENDING $M_h$

*Experimental ( $M_h$  tests).* Four specimens were subjected to horizontal moment combined with vertical pre-compression. Two specimens were tested at each of two levels of compressive force (nominally 1.25 and 2.5 kN). The specimens were constructed from the same solid clay bricks as the vertical bending tests but the mortar was a 1:1:6 with ten times the recommended dose of air entraining agent to create deliberately low bond strength (mean bond wrench flexural strength of 0.18 MPa, std dev. 0.05 MPa). This was done so that attention could be focussed on joint rather than brick failure. The specimen behaviour consisted of an essentially linear initial response followed by cracking of the perpend and bed joints. A softening response was then observed as torsional shearing of the bed joints occurred with increasing rotation. Finally the moment  $M_h$  reached a constant residual value due to the frictional behaviour of the cracked bed joints under the action of the vertical pre-compression. Table 1 lists the test results for peak and residual moments. While efforts were made to stabilise the compressive force, a small variation was still noticed.

**Table 1 – Horizontal Bending Test Result**

Specimen No	Compression Force at Peak Load (kN)	Peak Moment (kNm)	Compression Force at Residual Load (kN)	Residual Moment (kNm)
1	1.352	0.274	1.416	0.077
2	1.20	0.173	1.251	0.060
Average (1 & 2)	1.276	0.224	1.334	0.069
3	2.46	0.295	2.51	0.151
4	2.51	0.302	2.59	0.122
Average (3 & 4)	2.49	0.298	2.55	0.137

*Numerical Modelling ( $M_h$  tests).* Using the same finite element mesh as used for the  $M_v$  simulations, the numerical model was used to simulate the above  $M_h$  tests. For these preliminary tests, the only control tests conducted were bond wrench tests. Therefore, the only input parameter available for the numerical modelling was flexural tensile strength. Hence, the modelling strategy was to adjust the shear contact parameters to fit the experimental result at one compression level. The same parameters were then used as input to simulate the specimens and validate the model under the other compression level. Figure 10 shows the simulated specimens'



behaviour under two different pre-compression levels. Here a friction coefficient of  $\mu = 0.55$  and cohesive strength of  $c = 0.145$  MPa were obtained by fitting the model to the experimental data under a compressive force of 1.25 kN. Under this compressive force the model predicted a peak horizontal moment of 0.232 kNm and a residual moment of 0.061 kNm. Using the same  $\mu$  and  $c$  values and a compressive force of 2.5 kN, a peak horizontal moment of 0.287 kNm and a residual moment of 0.118 kNm were obtained. These values compare well with the experimental data listed in Table 1.

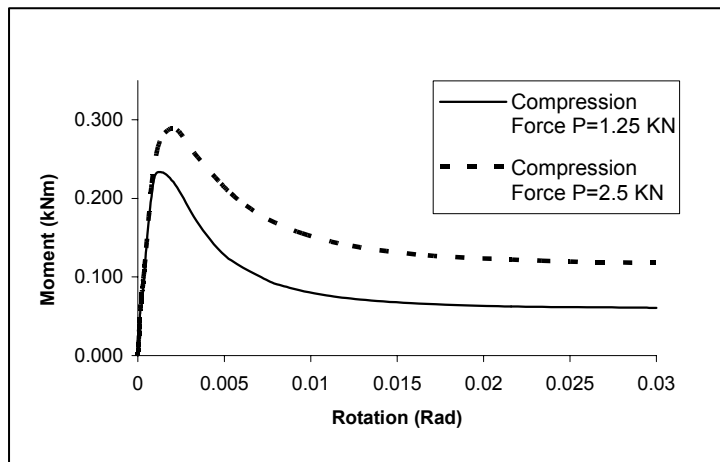


**Figure 10 – 4-Unit Specimens under Horizontal Bending**

Typical joint failure behaviour as predicted by the numerical model under horizontal bending is illustrated in Figure 11. To qualitatively validate the ability of the model to predict the brick failure mode, a modulus of rupture of 2.5 MPa (actual mean value of approximately 5 MPa) was applied to the brick/brick interface at the mid-length of the brick unit. Figure 12 demonstrates that for cases where the ratio of joint strength:brick strength is high the model is capable of capturing the failure by rupture of the bricks.

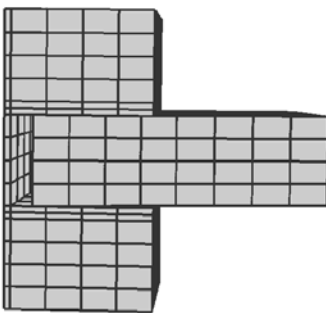


**Figure 11 – Joint Failure**

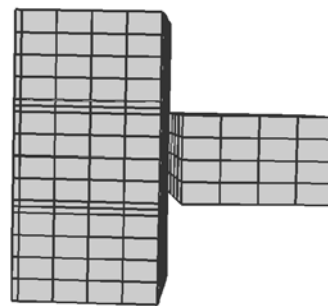


**Figure 12 – Brick Failure**

## CONCLUSION

A 3D non-linear finite element model capable of simulating the behaviour of masonry specimens under the simultaneous combination of horizontal and vertical bending moments and vertical compressive force was presented. The model was compared with preliminary experimental results separately for the cases of one way vertical bending and one way horizontal bending, each with various levels of vertical pre-compression. In the case of vertical bending, the model results,

together with an independent analytical approach, highlighted systematic errors in the experimental apparatus which are now being investigated. Under horizontal bending the model was able to duplicate the results of tests at one level of pre-compression after first fitting the model input parameters to test results under a lower level of pre-compression. Full validation of the model requires further experimental data, in particular, control tests to obtain model parameters, a greater number of 4-unit specimen replicates and tests in which vertical and horizontal bending moments are applied simultaneously.

## ACKNOWLEDGEMENTS

The authors wish to thank the laboratory staff of The School of Engineering, the University of Newcastle for their assistance in conducting the experiments. Yan Han would also like to thank Dr. Daichao Sheng for enlightening discussions, The University of Newcastle for the provision of a postgraduate scholarship, Austral Bricks Pty Ltd and the Clay Brick & Paver Institute (CBPI) for their funding contributions.

## REFERENCES

1. Han, Y. and Masia, M.J. A 3D Non-linear Finite Element Model of Brick Specimens Subjected to Bending. Proc. 7<sup>th</sup> Australasian Masonry Conference. Newcastle, Australia. 13-16 July 2004. pp. 446-455.
2. Lawrence, S.J. Behaviour of Brick Masonry Walls under Lateral Loading. PhD Thesis. University of New South Wales, Australia. 1983.
3. Lawrence, S.J. Lateral Loading of Masonry – An Overview. Proc. 3rd National Masonry Seminar. Brisbane, Australia. 14-15 July 1994. 20.1-20.9.
4. Baker, L.R. The Flexural Action of Masonry Structures under Lateral Load. PhD Thesis. Deakin University, Australia. 1981.
5. Fried, A.N., Roberts, J.J., Limbachiya, M.C., and Kanyeto, O. Predicting the Behaviour of Laterally Loaded Masonry Panels. Proc. 13<sup>th</sup> International Brick and Block Masonry Conference. Amsterdam. 4-7 July 2004.
6. Lawrence, S.J. and Marshall, R. Virtual Work Design Method for Masonry Panels under Lateral Load. Proc. 12<sup>th</sup> International Brick and Block Masonry Conference. Madrid, Spain. 25-28 June 2000.
7. Lotfi, H.R. and Shing, P.B. Interface Model Applied to Fracture of Masonry Structures. Journal of Structural Engineering. ASCE Vol. 120, No. 1, 1994. pp. 63-80.
8. Lourenco, P.B. and Rots, J.G. A Multi-Surface Interface Model for the Analysis of Masonry Structures. Journal of Engineering Mechanics. ASCE Vol. 123, No. 7, 1997. pp. 660-668.
9. Willis, C.R., Griffith, M.C., and Lawrence, S.J. Horizontal Bending of Face-Loaded Brick Masonry Wallettes. Proc. 6<sup>th</sup> International Masonry Conference. London. 4-6 November 2002.
10. Hibbit, Karlsson & Sorensen, Inc. Abaqus/Standard User's Manual, Version 6.3. Published by Hibbit, Karlsson & Sorensen, Inc., 2002. 1080 Main Street, Pawtucket, RI 02860-4847, United States.
11. Masia, M.J., Han, Y., Lawrence, S.J., and Page, A.W. An Experimental Study of Brick Masonry Specimens Subjected to Biaxial Bending. Proc. 13<sup>th</sup> International Brick and Block Masonry Conference. Amsterdam. 4-7 July 2004.
12. Standards Australia 2001, AS 3700-2001 – Masonry Structures. Published by Standards Australia International Ltd, GPO Box 5420, Sydney, NSW, Australia. 2001.